

Observation of Single Charge Carriers by Force Microscopy

C. Schönenberger^(a) and S. F. Alvarado

Zurich Research Laboratory, IBM Research Division, 8803 Rüschlikon, Switzerland

(Received 27 August 1990)

The scanning force microscope is used to deposit charge carriers on insulating Si_3N_4 films and to monitor their recombination. The charge decay shows up as a discontinuous staircase, demonstrating single-carrier resolution. The decay is found to be controlled by thermionic emission.

PACS numbers: 73.25.+i, 61.16.Di, 73.40.Bf, 73.50.Gr

The scanning force microscope (SFM) introduced by Binnig, Quate, and Gerber¹ is a remarkably useful instrument to map the surface topography of virtually any solid.² Most noticeably, atomic resolution has been achieved on insulating crystals.³ Besides the repulsive contact force used in profilometry, attractive forces like the quantum-mechanical exchange, electrostatic, and magnetic dipolar forces were utilized to measure such quantities as metallic adhesion,⁴ electric surface potential variation,⁵ and magnetic domain structures.⁶

In two recent Letters, Stern *et al.*⁵ and Terris *et al.*⁵ have demonstrated that the SFM can be used to deposit and image charges on insulators, both by contact electrification (CE) as well as by corona discharge (CD). They speculated that single carriers could be observable.

In this Letter the observation of single-charge recombination events is described. Ionized particles are deposited by a short CD (10 ms) onto silicon nitride (Si_3N_4) films prepared by plasma-enhanced chemical-vapor deposition (PECVD) onto degenerately doped (conducting) GaAs substrates. The detected charge signal following the CD was observed to decay within a few seconds in a staircase fashion, showing the charge quantization. The experiments described were performed in air at ambient conditions.

The force is detected with a differential interferometer described elsewhere.⁷ Figure 1 is a schematic of the tip apex, positioned at a distance d above an insulating film of thickness h . A voltage V applied to the tungsten tip

results in the Coulomb force $F=(V+\phi)^2G$, where G contains the tip radius R , d , and h , as well as the relative dielectric constant ϵ of the film. The term ϕ is the contact potential between the tip and sample. Applying an ac voltage $V=\sqrt{2}V_m\sin(\omega t)$ results in two measured oscillating force terms at ω and 2ω , with the respective rms amplitudes $F_1=2V_m\phi G$ and $F_2=V_m^2\sqrt{2}G$ from which G and ϕ can be extracted.⁸ The tip-to-sample distance d is adjusted by a controller loop so that F_2 and hence G remain constant. Since V_m and G are both constant, any contrast in F_1 is due to a varying contact potential ϕ . A charge carrier q lying on the surface of the insulator induces image charges q_i and q_i' in the tip and the substrate, respectively (Fig. 1). Since charge conservation requires $q_i+q_i'=-q$, the magnitude of q_i/q is always less than unity, increasing when the tip-sample distance d is decreased with respect to the film thickness h . The value of F_1 is approximately given by $F_1=q_iE_a$, where E_a is the rms electric field at the tip apex due to the applied ac voltage. In calculations, the dielectric constant ϵ can be taken into account by replacing h with the effective film thickness $h^*=h/\epsilon$. The effective tip-substrate distance is then given by $D=d+h/\epsilon$. This treatment is rigorous for homogeneous fields only. The field E_a is calculated for a tip modeled as a hyperboloid,⁹ having a fixed apex curvature of $1/R$:

$$E_a = \frac{V}{D} \frac{\sqrt{\xi(1+\xi)}}{\ln(\sqrt{\xi} + \sqrt{1+\xi})}, \quad (1)$$

with $\xi=D/R$. Moreover, G can be calculated for this geometry. For $D \ll R$, it follows that $G=\pi\epsilon_0R/D$. To calibrate the tip radius R , we measure $F_2(D)$ over a gold reference sample. Since the condition $D \ll R$ is not rigorously fulfilled within experimentally accessible distances of $D \geq 10$ nm, the slope $k=-\partial(\ln F_2)/\partial(\ln D)$ is found to be less than 1 (typically 0.3–0.6) with the tendency to increase at the smallest distances. Consequently, the tip radius $R(D)$, extracted from $F_2=\sqrt{2}V_m^2 \times \pi\epsilon_0R/D$ with the measured parameters F_2 , V_m , and D , is an upper bound to the real geometric R . A lower bound is found by extrapolating $R(D)$ to $D=0$.

The underlying insulating film is charged by applying a large dc voltage (≈ 10 V) to the tip for 10 ms. The

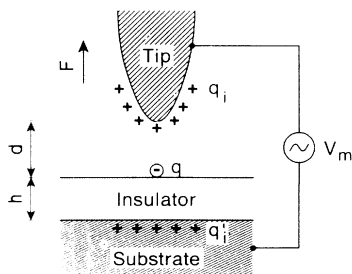


FIG. 1. Schematic explaining the detection of the excess charge q on an insulating film via the force F_1 related to the image charge q_i .

decay of the deposited charge is registered by the change in the force signal F_1 . The current tip-sample distance is frozen by inhibiting the controller loop during the period starting shortly before the voltage pulse and lasting until the end of the F_1 registration, which is typically a duration of 10 s. The value of F_2 remained constant during this period. The force signal F_1 is detected in an effective bandwidth of 5 Hz; hence, the time resolution is limited to about 30 ms. The background noise measured at a tip-sample distance $d \approx 100$ nm is smaller than 1 pN.¹⁰ The threshold voltage for discharge (6–30 V) as a function of d is found to be consistent with a constant threshold field of $\approx 6 \times 10^8$ V/m. Figure 2 shows two examples of the subsequent decay of F_1 as a function of time t , obtained on a Si_3N_4 film of thickness $h = 20$ nm, with the parameters $d = 25$ nm, $R = 40 \pm 20$ nm, and $E_a = (1.5 \pm 0.4) \times 10^8$ V/m. The discharge voltage was +8 V for both examples; hence, the underlying surface was positively charged. The decays of the deposited positive charge are seen to be discontinuous, with clearly resolved plateaus. The axis denoted by f on the right of Fig. 2 is a scale $f = F_1/eE_a$ for the expected step size for one elementary unscreened charge in the field E_a . The contribution to the force by charge carriers located on the insulator surface depends on their position with respect to the tip apex. The measured step size $s = \Delta f$ is therefore not constant. The step size s is found to be 0.1 ∓ 0.04 , and hence the image charge is $q_i \approx e/10$. A value of q_i was calculated for a spherical tip above a conducting sample, with the charge q located between the tip and sample at a height of $h^* = h/\epsilon$ above the sample surface. For the experimental parameters, and with $\epsilon = 4$, we obtain the theoretical value $s_{\text{th}} = 0.13$, in good agreement with experiment. However, s_{th} should be compared with the largest measured step size and not with the mean value as we have done. This is hindered by the limited time resolution which does not allow the largest measured step size to be identified unambiguously. Apart from this problem, the comparison between s

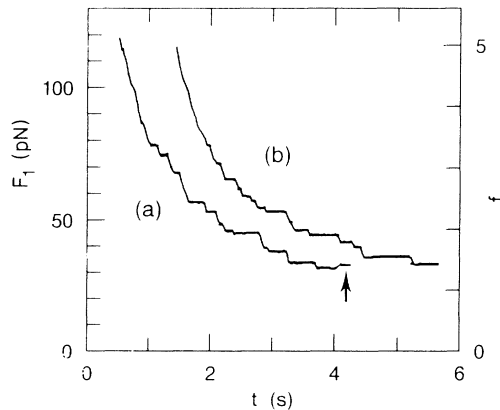


FIG. 2. Trace a , force F_1 vs time t for a positively charged 20-nm-thick Si_3N_4 film. Trace b is shifted to the right by 1 s.

and s_{th} is subject to an error of about 60% due to uncertainties in E_a and the calculated image charge.

At the end of trace a in Fig. 2 a step—marked with an arrow—is seen to go in the opposite direction. Apparently this step is not driven by the electric field established in the tip-sample region due to the presence of the charge. Such steps going up and down are also seen without any excitation. They appear, however, at a lower rate than the steps found in the charge decay. Moreover, with increasing tip-sample distance the step height is found to decrease as does the rate of appearance. These observations indicate that the observed process might be driven by thermal activation.

For the thicker (200 nm) insulator, larger steps are expected to occur since the substrate electrode is farther away from the charge q , and hence the image charge q_i in the tip is increased. This is shown in Fig. 3 for the experimental parameters $d = 50$ nm, $R = 100 \pm 40$ nm, and $E_a = (0.6 \pm 0.2) \times 10^8$ V/m. The deposited charge is of positive sign again and was obtained with a discharge voltage of +20 V. The step size s deduced from this figure is between 0.4 and 0.9 and $s_{\text{th}} = 0.5$, obtained as before.

The larger step size obtained on the thicker insulating film supports our view that the steps are due to single-charge recombination on the insulating surface. In accordance with this view is the observation that the measured step size decreases with increasing tip-sample distance d even if the apex field E_a is kept constant. This is due to the lowering of the image charge in the tip which occurs when d is increased. In a control experiment performed on the conducting substrate with the same charging procedure, no charge transfer was found within the given time resolution.

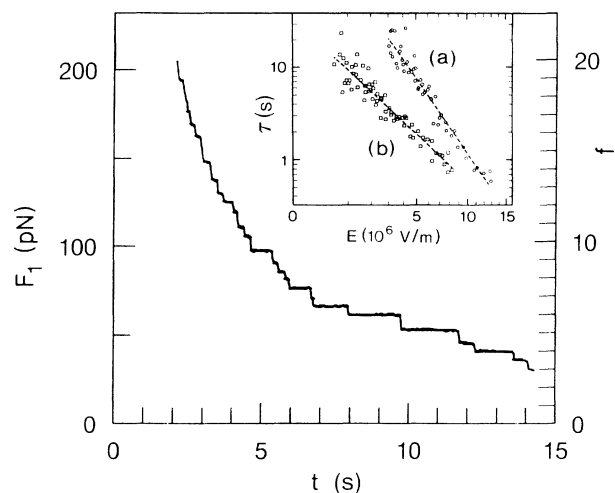


FIG. 3. Force F_1 vs time t for a positively charged 200-nm-thick Si_3N_4 film. Inset: The time constant τ of several measured decays as a function of the electric field E as described in the text.

Apart from the steps, the decay is not exponential. The decay time $\tau = -F_1/(\partial F_1/\partial t)$ increases with t . This suggests a field-dependent process that could be either tunneling, field emission, or thermionic emission.¹¹ The strongest field in the tip-sample region is caused by the applied modulation voltage: $E_a \approx 10^8$ V/m. If tunneling or field emission were the dominating process, the decay would be strongly dependent on V_m , much more than it would be for thermionic emission. We found the decay rate to be independent of V_m , for $V_m = 2-6$ V. For thermionic emission, τ is given by¹²

$$\tau = AT^2 \exp\left(\frac{-\Phi + \beta\sqrt{E}}{kT}\right), \quad (2)$$

where Φ is the barrier height, E is the electric field between tip and sample, and the constant $\beta = 6 \times 10^{-24}$ (mks) for Schottky emission. Depending on the sign of the charge carriers on the insulator, two different lines are found in the $\ln(\tau)$ vs \sqrt{E} plot (inset of Fig. 3), where the electric field E is generated by the charge and its image charges. The value of E is calculated from $E = F_1/\epsilon_0 A E_a$ with the effective tip area A taken to be $R^2\pi$. For positive deposited charge, trace b in the inset, we find $\beta^+ = 5.4 \times 10^{-24}$ (mks), and for negative charge, trace a in the inset, $\beta^- = 8 \times 10^{-24}$ (mks). This is in reasonable agreement with the theoretical value for Schottky emission.¹² The two curves allow the barrier height Φ to be estimated. Taking 100 initially deposited carriers, an initial decay time τ of 0.4 s, and a field of $E = 14 \times 10^6$ V/m yields a barrier height of 0.95 eV. For such a barrier and tip-sample distances of $d \geq 20$ nm, the tunneling probability is much smaller than the thermally activated hopping over the barrier. Positive charge deposited onto the insulating surface is therefore recombined by thermionic emission of electrons from the tip, whereas for deposited charge of negative-sign electrons have to jump back to the tip by thermal activation.

In conclusion, single-charge-carrier recombinations were detected on Si_3N_4 films, demonstrating the force microscope's unique capability of high-resolution potentiometry. The possibility of counting single electrons or measuring a current of the order of 0.1 aA makes possible a variety of experiments in combination with tunneling, e.g., investigation of charge quantization in small tunnel capacitors and in resonant structures.¹³ Moreover, the statistics of tunneling emission can be studied. To ensure that tunneling dominates over thermionic emission, the barrier size Φ (1 eV in our experiments) could be increased, d could be reduced, or the experiment

could be done at lower temperatures.

We thank H. Rohrer, E. Courtens, and U. Dürig for support, motivation, and the necessary freedom. Stimulating discussions with D. Abraham, P. Renaud, and M. Lutz, advice on chemistry by B. Michel and L. Häussling, as well as the film preparation by E. Marclay, D. Webb, and K. Dätwyler are all gratefully acknowledged.

^(a)Present address: Philips Research, P.O. Box 80.000, 5600 JA Eindhoven, The Netherlands.

¹G. Binnig, C. F. Quate, and Ch. Gerber, *Phys. Rev. Lett.* **56**, 930 (1986).

²P. K. Hansma, V. B. Elings, O. Marti, and C. E. Bracker, *Science* **242**, 209 (1988), and references therein.

³T. R. Albrecht and C. F. Quate, *J. Appl. Phys.* **62**, 2599 (1987); E. Meyer, H. Heinzelmann, H. Rudin, and H.-J. Güntherodt, *Z. Phys. B* **79**, 3 (1990).

⁴U. Dürig, O. Züger, and D. W. Pohl, *Phys. Rev. Lett.* **65**, 349 (1990).

⁵Y. Martin, D. W. Abraham, and H. K. Wickramasinghe, *Appl. Phys. Lett.* **52**, 1103 (1988); J. E. Stern, B. D. Terris, H. J. Mamin, and D. Rugar, *Appl. Phys. Lett.* **53**, 2717 (1988); B. D. Terris, J. E. Stern, D. Rugar, and H. J. Mamin, *Phys. Rev. Lett.* **63**, 2669 (1989).

⁶Y. Martin and H. K. Wickramasinghe, *Appl. Phys. Lett.* **50**, 1455 (1987); C. Schönenberger and S. F. Alvarado, *Z. Phys. B* **80**, 373 (1990); D. Rugar, H. J. Mamin, P. Guethner, S. E. Lambert, J. E. Stern, I. McFadyen, and T. Yogi, *J. Appl. Phys.* **68**, 169 (1990), and references therein.

⁷C. Schönenberger and S. F. Alvarado, *Rev. Sci. Instrum.* **60**, 3131 (1989).

⁸B. D. Terris, J. E. Stern, D. Rugar, and H. J. Mamin, *J. Vac. Sci. Technol. A* **8**, 374 (1988).

⁹P. Moon and D. E. Spencer, *Field Theory for Engineers* (Van Nostrand, Princeton, NJ, 1961).

¹⁰The thermal fluctuations in the cantilever correspond to a background force of ≤ 0.5 pN (Ref. 7) for the following typical measurement conditions: bandwidth 5 Hz, cantilever compliance 10–20 N/m, and a cantilever resonance frequency of 10 kHz.

¹¹R. Coelho, *Physics of Dielectrics* (Elsevier, New York, 1979); G. M. Sessler, B. Hahn, and D. Y. Yoon, *J. Appl. Phys.* **60**, 318 (1986).

¹²V. M. Efimov, V. A. Kolosonov, and S. P. Sinitsa, *Phys. Status Solidi (a)* **49**, 217 (1978); J. G. Simmons, *Phys. Rev.* **155**, 657 (1967).

¹³J. Lambe and R. C. Jaklevic, *Phys. Rev. Lett.* **22**, 1371 (1969); P. J. M. van Bentum, H. van Kempen, L. E. C. van de Leemput, and P. A. A. Teunissen, *Phys. Rev. Lett.* **60**, 369 (1988); F. Guinea and N. Garcia, *Phys. Rev. Lett.* **65**, 281 (1990).

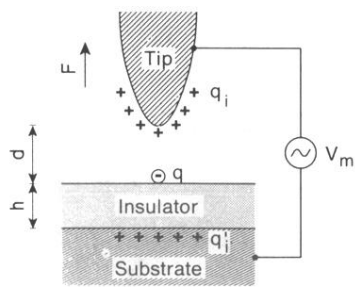


FIG. 1. Schematic explaining the detection of the excess charge q on an insulating film via the force F_1 related to the image charge q_i .